

Laser micro-drilling of CNT reinforced polymer nanocomposite: A parametric study using RSM and APSO

Lipsamayee Mishra^{1a}, Trupti Ranjan Mahapatra^{*1}, Debadutta Mishra^{1b}
and Akshaya Kumar Rout^{2c}

¹Department of Production Engineering, Veer Surendra University of Technology, Burla, 768018, India

²School of Mechanical Engineering, KIIT Deemed to be University, Bhubaneswar, 751024, India

(Received March 5, 2022, Revised June 18, 2023, Accepted July 10, 2023)

Abstract. The present experimental investigation focuses on finding optimal parametric data-set of laser micro-drilling operation with minimum taper and Heat-affected zone during laser micro-drilling of Carbon Nanotube/Epoxy-based composite materials. Experiments have been conducted as per Box-Behnken design (BBD) techniques considering cutting speed, lamp current, pulse frequency and air pressure as input process parameters. Then, the relationship between control parameters and output responses is developed using second-order nonlinear regression models. The analysis of variance test has also been performed to check the adequacy of the developed mathematical model. Using the Response Surface Methodology (RSM) and an Accelerated particle swarm optimization (APSO) technique, optimum process parameters are evaluated and compared. Moreover, confirmation tests are conducted with the optimal parameter settings obtained from RSM and APSO and improvement in performance parameter is noticed in each case. The optimal process parameter setting obtained from predictive RSM based APSO techniques are speed=150 (m/s), current=22 (amp), pulse frequency (3 kHz), Air pressure (1 kg/cm²) for Taper and speed=150 (m/s), current=22 (amp), pulse frequency (3 kHz), air pressure (3 kg/cm²) for HAZ. From the confirmatory experimental result, it is observed that the APSO metaheuristic algorithm performs efficiently for optimizing the responses during laser micro-drilling process of nanocomposites both in individual and multi-objective optimization.

Keywords: accelerated particle swarm optimization; CNT/Epoxy based PMC; heat-affected zone; laser micro-drilling; RSM; taper

1. Introduction

Laser beam machining (LBM) is a fast way to machine advanced engineered materials such as metals, nonmetals, ceramics, composites, and alloys (Meijer 2004). As a result, it is the best instrument for precision micro-drilling operations on a variety of objects ranging from turbine blades, watches to circuit boards. In the laser beam micro-drilling (LMBD) process, a laser beam source removes material from the work piece when a high intensity, directional coherent

*Corresponding author, Associate Professor, E-mail: trmahapatra_pe@vssut.ac.in

^aPh.D., E-mail: mishra.lipsa13@gmail.com

^bPh.D., E-mail: dmvssut@gmail.com

^cPh.D., E-mail: akshayakumarrou@vssut.ac.in

monochromatic beam is directed on a very small spot, it causes vaporization, melting, and chemical degradation over the whole depth of the material, resulting in the formation of a hole. The coaxial assist gas jet with the laser beam aids in the removal of fluids, speeds up the treated material, and expels it from the machining region (Goswami and Chakraborty 2015). LBMD leads to no mechanical damage, a high production rate, low tool wear due to non-contact processing, applicability to both conductive and non-conductive materials, minimal material waste, narrow heat-affected zone (HAZ), high surface finish, improved product quality, and environmentally clean technology. It has a wide range of applications in the marine, aeronautics, aerospace, and automotive industries. The CO₂ lasers and the Nd:YAG lasers are the most often utilized lasers among the many types of lasers (Kumar and Gururaja 2020). Nd:YAG lasers lead the drilling industry due to their high average power and convenience (compactness, low cost, and multiple suppliers) (Chien and Hou 2007).

Carbon is the sixth element in the periodic table, and its different forms such as diamond, graphite, carbon black, charcoal, and conjugated carbon nanomaterials such as carbon nanotubes and fullerenes have been employed as energy sources due to their unique qualities. Material at nano scale are known to exhibit unique physic-chemical properties that are not found in its bulk counterpart (Gao *et al.* 2014, Masir *et al.* 2018, Sharon *et al.* 2017). The carbon nanotubes (CNTs), when compared to other carbon materials, are found to be the best reinforcements in composites due to a wide range of applications ranging from microelectronics to the aerospace industry due to high tensile strength (10 GPa), high modulus of about 1 TPa, and low density of 2.1 g/cm³ (Singh and Aul 2021). A number of nanocomposites have been created by embedding CNT filler into various polymer matrices such as epoxy, polypropylene (PP), and polyamides. Epoxy resin is a powerful polymer matrix that is commonly used to reinforce nanotubes (Wang and Chen 2014). This type of matrix has a startling specific strength, stiffness, and chemical affinity for the filler components (Ahmed *et al.* 2015). Because of its customized mechanical and chemical qualities, epoxy resin has been favored for a variety of structural as well as microelectronics applications (George *et al.* 2013). However, traditional machining of such materials is problematic because of properties like brittleness, anisotropy, and non-homogeneity. Due to the vast range of uses of nanocomposite, micro-drilling is required for assembling numerous components, which is almost impossible using the usual drilling approach. According to the findings of a specific study, conventional procedures have an impact on the work piece through chipping, cracking, delamination, and impact damage on the cutting tool (Patel *et al.* 2013). Researchers discovered that polymer matrix composites can be easily machined utilizing unconventional machining processes. Among the several non-traditional machining technologies accessible, electro discharge machining is intended for electrically conductive materials. Abrasive jet and water jet machining can be tailored for fragile materials, and ultrasonic machining can be used for tougher materials, but laser machining is a non-contact, abrasion-free technology that reduces tool wear and can be used for practically any type of material. The laser micro-drilling technique, a non-conventional drilling method, is the most ideal approach for micro-drilling operation on diverse components ranging from turbine blades to watches to circuit boards (Galińska 2020). Machining is achieved in a non-contact type thermal energy-based machine by directing a stream of plasma, photons, positive ions, and electrons onto the work piece surface. Due to advantages such as high accuracy and repeatability, laser drilling is a less expensive and more controllable alternative to Computer Numerical Control (CNC) drilling, punching, wire electro discharge machining (EDM), broaching, and other prominent destructive hole drilling technologies (Jain *et al.* 2019, Mishra *et al.* 2020, Rajesh *et al.* 2017, Saini and Dubey 2019).

To get the most out of these machining processes, the system engineers look for an optimal

collection of parameters that offer the best outcomes under various processing restrictions. However, different conventional techniques such as weighted signal-to-noise (WSN) ratio, Grey Relational Analysis (GRA), multiple-response signal-to-noise (MRSN) ratio, VIKOR (Vise Kriterijumska Optimizacija I Kompromisno Resenje in Serbian), and weighted principal component (WPC) methods (Gauri and Pal 2010) have been developed to optimize multiple responses. However, these strategies are irrational when the process parameter variable is not continuous as they can only find the best set within the parameter level combinations defined for the process. This makes non-traditional methods such as genetic algorithm (GA), particle swarm optimization algorithm (PSO), artificial neural network (ANN) technique, Tabu search algorithm (TS), and ant colony algorithm (ACO) more popular for determining the set of optimal process parameters in multi-response optimization. To solve multi-objective problems, Liu et al. (2021) used a multi-objective genetic algorithm to investigate the effects of scanning speed, pulse frequency, pulse width on taper and heat affected zone to achieve high quality micro-holes on 2.5D C_f/SiC composite. Biswas *et al.* (2010) investigated the characterization of hole circularity at entry and exit, taking into account process parameters such as pulse width, air pressure, lamp current, pulse frequency, and focal length. Kuar et al. (2008) used response surface methodology (RSM) and a hybrid Taguchi technique for multi-objective optimization of laser cutting processes using input parameters such as pulse frequency, cutting speed, pulse width, and assist gas pressure. Rao and Yadava (2009) established a hybrid optimization approach for determining ideal laser cutting process parameters using input factors such as pulse frequency, pulse width, oxygen pressure, and cutting speed to optimize kerf width, kerf deviation, and kerf taper. Adalarasan et al. (2017) have studied the optimal machining parameters in pulsed CO₂ laser cutting of Al6061/Al₂O₃ composite using Taguchi-based response surface methodology. From the study, it is concluded that lower level of pulse frequency resulting in a better surface finish due to excessive melting and re-solidification. Yan et al. (2012) have performed combined experimental and numerical study on laser percussion drilling of thick section alumina. The study suggested that the size and temperature of the melt front significantly affected the hole diameter formation and spatter deposition during laser percussion drilling. Sibalija et al. (2011) created a strategy for the hybrid design of optimal laser drilling parameters that optimize the responses of the drilled holes. Ciurana et al. (2009) minimized surface roughness and volume inaccuracy in laser micromachining using PSO-based multi-objective optimization. Using design of experiments (DOE) and the GRA, Nagesh et al. (2013) investigate the effect of carbon nano powder/vinyl ester/glass nanocomposites on the HAZ and the taper angle of a laser-drilled hole using laser parameters such as pulse frequency, laser power, and scanning velocity. Gautam and Mishra (2019) investigated the effects lamp current, pulse frequency, pulse width air pressure and cutting speed on kerf deviation, kerf width and kerf taper using a multi objective firefly algorithm. Muthukumar et al. (2015) optimized parameters in the wire EDM process using a multi-objective evolutionary GA. Yan et al. (2012) studied the impact of laser peak power, pulse repetition rate, and pulse duty cycle on hole diameter creation and spatter deposition during laser percussion drilling. Mukherjee et al. (2013) compared the artificial bee colony (ABC) method to other population-based algorithms such as particle swarm optimization, the genetic algorithm, and the ant colony optimization algorithm. T-test findings show that the ABC method is superior to the other optimization algorithm. Chatterjee et al. (2018) used an evolutionary approach (GA) to determine the best drilling parameter settings. According to the findings, increasing laser intensity leads to increased HAZ and circularity error.

Pulsed Nd: YAG Laser offers an attractive alternative for various micro-machining operations of a wide range of advanced engineering materials like metals, nonmetals, ceramics, composites and

alloys. However, achieving good quality holes in composite material, with low taper, low HAZ, and high material removal rate (MRR) is a difficult issue. This is because, when the laser's input energy is high, the work piece is over burned at the required hole, and the excess material is removed from the required cross-section, resulting in dimensional inaccuracies and a decrease in hole quality in terms of taper and HAZ. As a result, it is critical to select appropriate laser process parameters to produce high-quality holes during micro-drilling operations.

Based on previous research, it is clear that the use of polymer matrix composite materials in laser drilling operations is less outlined and efforts to drill a quality hole with optimal parameter settings are still relatively limited. Moreover, the PSO model is found to provide an excellent correlation with the experimental data as compared to the RSM model (Suhaimi et al. 2019). Therefore, the current research aims to use a recently developed metaheuristic Accelerated Particle Swarm Optimization (APSO) algorithm to estimate the optimal set of laser micro-drilling process parameters that produce the minimum taper, and minimum HAZ for a polymer matrix nanocomposites. In order to reduce the time and cost, the experimentation is planned as per the BOX-Behnken design (BBD) based on the RSM and the significant controllable parameters are identified. Micrograph analysis has been carried using scanning electron microscope (SEM) to calculate the hole taper and HAZ. The optimal controllable parameters are attained by considering the taper and HAZ as the performance indicators and validated via confirmation runs. Comparative analysis is also made between the results obtained from the RSM analysis and the APSO for both single objective and multi-objective cases, to assess the efficacy of each methodology in multiple performance optimization during pulsed Nd: YAG micro-drilling of CNT-based polymer nanocomposites.

2. Experimental planning

2.1 Work piece materials

In order to conduct the experiments a polymeric composite with carbon nanotube (CNT, 95%, OD 20-30 nm, length 10-30 μm) as fillers with viscous epoxy-based polymer matrix laminate specimens of 3mm thickness is prepared. The epoxy (61.5625 g) used as the matrix material, is a class of reactive polymer containing the epoxide group. When reacted with hardeners by

Table 1 Chemical composition of work material's elements weight % used in experimentation

Elements	C	O	Na	Si	S	Cl	K	Zn
Weight%	80.43	17.35	0.12	0.96	0.10	0.62	0.09	0.33

Table 2 Characteristics of the prepared CNT/epoxy-based polymer nanocomposite

Characteristics	Unit	Value	Characteristics	Unit	Value
Glass transition temperature	$^{\circ}\text{C}$	312.14	Tensile properties		
Thermal conductivity	W/m-K	0.1832	Young's modulus	MPa	4050
Electrical conductivity	S/m	2.1×10^{-5}	Ultimate tensile strength	MPa	78
Microhardness	N/mm ²	17.34	Ultimate tensile strain	(%)	5.8

curing/crosslinking reaction to form thermosetting polymers, it offers high mechanical and thermal properties. The laminated composite is fabricated using traditional hand lay-up technique assisted with an Ultrasonicator (Make: LABMAN, 2.5L) for uniform mixing of the CNT fillers in the epoxy matrix. In the present analysis, a Sonics Vibra Cell liquid processor is used for the sonication (Ti-horn, frequency of 20 kHz). The mixing beaker is used to avoid a temperature rise during sonication. To determine the optimal parameter (Total energy) sonication parameters like variety of mixing times and amplitudes have been examined. The sonication processor continuously displays the actual amount of power that is being delivered to the probe. The chemical composition of the presently prepared CNT/Epoxy composite is evaluated through Energy Dispersive X-Ray (EDX) analysis and depicted in Table 1. The corresponding thermal, electrical and mechanical properties are also acquired and provided in Table 2.

2.2 Experimental procedure

The micro-drilling of the currently prepared polymer nanocomposite is performed on a pulsed CNC Nd:YAG laser micro-machining system, designed by Sahajanand Laser Technology India (Fig. 1) having wavelength 1064 nm, laser beam spot diameter of 100 μm , average power 75 watts, beam diameter 1 mm, pulse width 120 ns and focal length of the focusing lens 77 mm. Pulsed CNC Nd: YAG laser system including beam delivering unit, power supply unit, radio frequency (RF) Q-switched driver unit, cooling unit and other subsystems driven through CNC controller for X-Y-Z axis movement is employed throughout this experimental investigation. A krypton (kr) arc lamp is utilized as a pumping source for Nd: YAG crystal. The laser beam's energy is regulated by means of the current supply to the lamp. The capability of delivering maximum average power (in pulsed mode) is about 25 W. Nozzle diameter, focal length of the lens, Nozzle standoff distance and thickness of the workpiece material are maintained constant during the experimentation.

2.3 Process parameters and experimental design

Among diverse factors those affect the machining efficiency in laser beam machining, the cutting speed, lamp current, pulse frequency and assist air pressure have a significant influence on the taper



Fig. 1 Nd:YAG laser micro-drilling machine setup

Table 3 Laser micro-drilling factors and their levels

Symbol	Cutting factors	Level 1	Level 2	Level 3
X_1	Cutting Speed (m/s)	30	90	150
X_2	Lamp Current (amp)	22	24	26
X_3	Pulse frequency (kHz)	3	9	15
X_4	Air pressure (kg/cm ²)	1	3	5

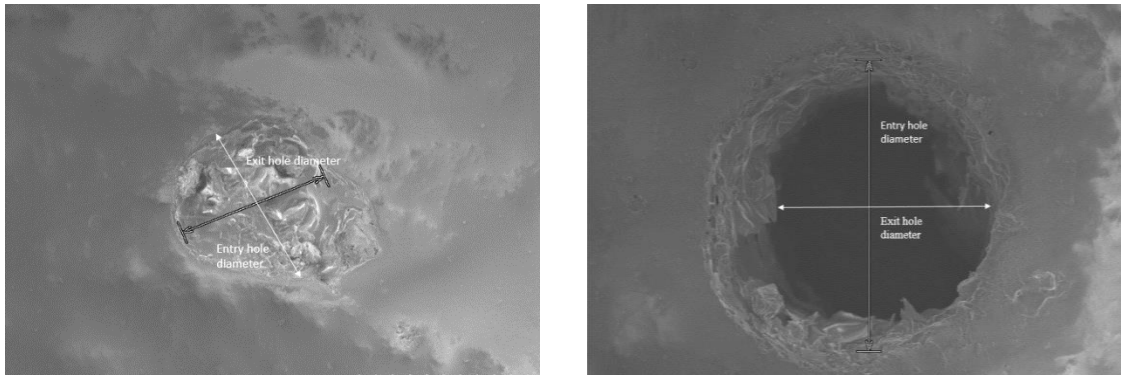


Fig. 2 SEM image of the worst hole and best hole obtained from the experiment

and HAZ. The process parameters are selected as per the accessibility of controllable range for each parameter in the laser machine and the levels of process parameters chosen alongside their notations used in the present study are shown in Table 2. An effective plan, Box-behnken design based on response surface methodology (Kipfer 2021), is used for planning and conducting experiments so as to establish the mathematical relationship between the response and the various machining parameters. The summary of the experimental results is depicted in Table 3. Work sample is mounted on machining table of the laser machining system with the help of developed work holding fixture. After conducting the experiments, the hole quality characteristics such as the hole entrance diameter, hole exit diameter, and width of HAZ are measured using a scanning electron microscope (SEM). The SEM images of the best hole and worst hole obtained from the experiment is provided in Fig. 2. The taper angle is calculated as

$$\left(\text{Taper}(\text{degree}) = \tan^{-1} \left\{ \frac{(d_{ent} - d_{exit})}{2 \times \text{thickness of material}} \right\} \times \frac{180}{\pi} \right) \quad (1)$$

Where, d_{ent} and d_{exit} are the entrance hole and exit hole diameter, respectively and the thickness of material=3 mm.

2.4 Research methodology

The steps employed in this research work are summarized below:

- Step 1: Related control parameters are chosen and the output responses are acquired according to BBD matrix based on the RSM.
- Step 2: Ideal combinations of optimal parameter setting are determined to optimize the individual responses and assess their significance through regression models using MINITAB statistical software.

Table 4 Experimental details and responses

Sl. No.	Cutting Speed X_1 (m/s)	Lamp Current X_2 (amp)	Pulse frequency X_3 (kHz)	Air pressure X_4 (kg/cm ²)	Taper (degree)	HAZ (μ m)
1	30	22	9	3	2.38	308
2	150	22	9	3	4.27	482
3	30	26	9	3	2.97	322
4	150	26	9	3	4.84	505
5	90	24	3	1	2.5	273
6	90	24	15	1	6.26	653
7	90	24	3	5	2.32	291
8	90	24	15	5	6.34	632
9	30	24	9	1	3.51	513
10	150	24	9	1	5.65	530
11	30	24	9	5	4.94	503
12	150	24	9	5	5.89	514
13	90	22	3	3	1.08	230
14	90	26	3	3	2.27	256
15	90	22	15	3	4.94	604
16	90	26	15	3	6.84	685
17	30	24	3	3	2.38	157
18	150	24	3	3	3.05	193
19	30	24	15	3	5.42	624
20	150	24	15	3	6.56	643
21	90	22	9	1	3.65	461
22	90	26	9	1	4.57	445
23	90	22	9	5	3.82	365
24	90	26	9	5	4.62	452
25	90	24	9	3	4.57	442
26	90	24	9	3	4.53	397
27	90	24	9	3	4.10	410

• Step 3: APSO algorithm is implemented to optimize the laser beam machining process parameters for which the regression equations, as developed in step 2, serves as the basic objective function by taking the current research into account (i.e., minimization of taper, minimization of the heat-affected zone).

• Step 4: In the last step, the optimized values obtained using RSM and APSO are evaluated by conducting the confirmatory test.

3. Results and discussion

3.1 Evolution of regression models using RSM

Table 5 Regression equation for the taper and HAZ during the Laser beam drilling process

Responses	Regression equation (In terms of coded factors)
Taper (Y_1)	$Y_1 = -93.6 + 0.0140X_1 + 7.70X_2 - 0.001X_3$ $-0.09X_4 + 0.000020X_1^2 - 0.1575X_2^2 - 0.00462X_3^2$ $+0.0869X_4^2 - 0.00004X_1X_2 + 0.000326X_1X_3$ $-0.00248X_1X_4 + 0.0148X_2X_3 - 0.0075X_2X_4 + 0.0054X_3X_4$
HAZ (Y_2)	$Y_2 = -1030 - 0.21X_1 + 124X_2 + 8.1X_3 - 230X_4$ $+ 0.00284X_1^2 - 3.04X_2^2 + 0.100X_3^2 + 13.11X_4^2 + 0.019X_1X_2$ $- 0.0118X_1X_3 - 0.012X_1X_4 + 1.15X_2X_3 + 6.44X_2X_4 - 0.81X_3X_4$

Table 6 Regression analysis for taper and HAZ

Source	Taper						HAZ					
	DF	Adj SS	Adj MS	F-Value	P-Value	% Contribution	DF	Adj SS	Adj MS	F-Value	P-Value	% Contribution
Model	14	57.4237	4.1017	18.21	0.000	95.504	14	541812	38701	11.4	0.000	93.006
Linear	4	52.6548	13.1637	58.43	0.000	87.572	4	517686	129421	38.12	0.000	88.864
X_1	1	6.2496	6.2496	27.74	0.000	10.394	1	16133	16133	4.75	0.05	2.769
X_2	1	2.9701	2.9701	13.18	0.003	4.940	1	3852	3852	1.13	0.308	0.661
X_3	1	43.1681	43.1681	191.62	0.000	71.795	1	496540	496540	146.23	0.000	85.234
X_4	1	0.267	0.267	1.19	0.298	0.444	1	1160	1160	0.34	0.570	0.199
Square	4	4.213	1.0532	4.68	0.017	7.007	4	20236	5059	1.49	0.266	3.474
X_1^2	1	0.0271	0.0271	0.12	0.735	0.045	1	556	556	0.16	0.693	0.095
X_2^2	1	2.1168	2.1168	9.4	0.010	3.521	1	789	789	0.23	0.638	0.135
X_3^2	1	0.1474	0.1474	0.65	0.434	0.245	1	68	68	0.02	0.889	0.012
X_4^2	1	0.644	0.644	2.86	0.117	1.071	1	14677	14677	4.32	0.060	2.519
2-Way Interaction	6	0.5559	0.0926	0.41	0.858	0.925	6	3890	648	0.19	0.973	0.668
X_1X_2	1	0.0001	0.0001	0	0.984	0.000	1	20	20	0.01	0.94	0.003
X_1X_3	1	0.0552	0.0552	0.25	0.629	0.092	1	72	72	0.02	0.886	0.012
X_1X_4	1	0.354	0.354	1.57	0.234	0.589	1	9	9	0	0.960	0.002
X_2X_3	1	0.126	0.126	0.56	0.469	0.210	1	756	756	0.22	0.645	0.130
X_2X_4	1	0.0036	0.0036	0.02	0.901	0.006	1	2652	2652	0.78	0.394	0.455
X_3X_4	1	0.0169	0.0169	0.08	0.789	0.028	1	380	380	0.11	0.744	0.065
Error	12	2.7034	0.2253			4.496	12	40747	3396			6.994
Lack-of-Fit	10	2.5676	0.2568	3.78	0.227	4.270	10	39674	3967	7.4	0.125	6.810
Pure Error	2	0.1358	0.0679			0.226	2	1073	536			0.184
Total	26	60.1271				100	26	582558				100

The RSM is a set of mathematical approach that is helpful for modeling and analyzing the relationship between several explanatory variables with one or more response variables. To obtain a fit model equation for a greater number of significant terms which can explain response in an improved way with less error and high R^2 value, the 2nd order regression equation is expressed as:

Table 7 Summary of regression analysis

Responses	S-value	R ² (%)	Adjusted R ² (%)	R ² (Pred)
Taper	0.474638	95.50%	90.26%	74.90%
Heat affected zone	58.2713	93.01%	84.85%	60.36%

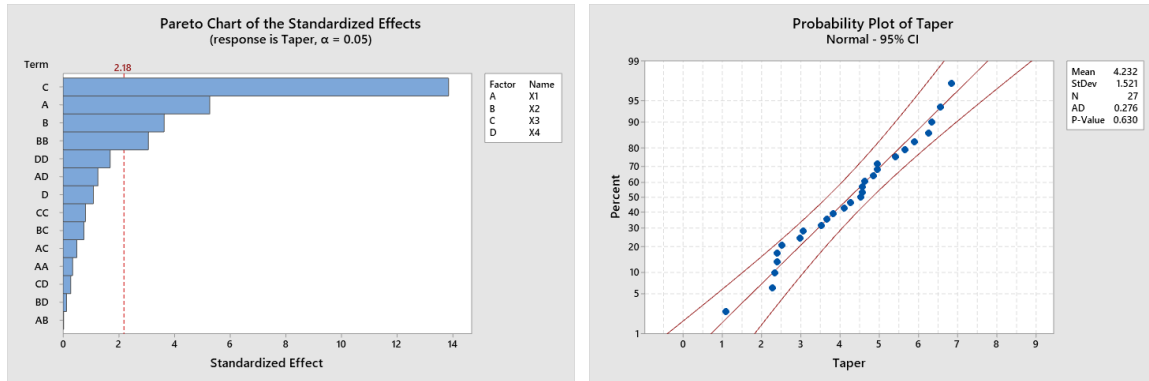


Fig. 3 Pareto chart of the standardized effects and probability plot of residuals for taper

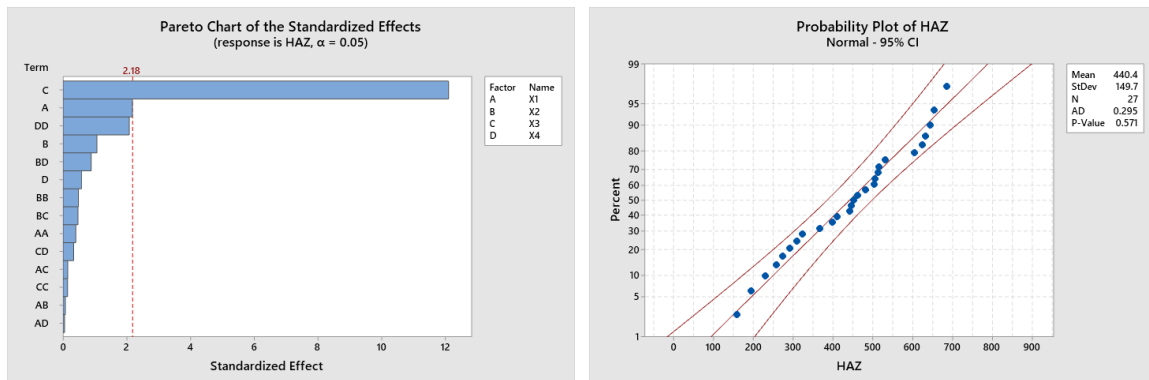


Fig. 4 Pareto chart of the standardized effects and probability plot of residuals for HAZ

$$y = \beta_0 + \sum_{i=1}^k \beta_i x_i + \sum_{i=1}^k \beta_{ii} x_i^2 + \sum_{i < j} \beta_{ij} x_i x_j + E \tag{2}$$

where y is the response function, β_0 is the intercept, $\sum_{i=1}^k \beta_i x_i$ is the main effect, $\sum_{i=1}^k \beta_{ii} x_i^2$ is the quadratic effect term, $\sum_{i < j} \beta_{ij} x_i x_j$ is the interaction terms effect and E is the error term.

In the present study, BBD in RSM is used to obtain the DOE and a total of 27 combinations are obtained for the drilling operation as mentioned in Table 4. Further, MINITAB Statistical Software has been used for the analysis purpose. The mathematical relations are established for correlating the process variables with the responses (Kuar et al. 2010). Table 5 shows the regression models thus obtained.

The acceptability of the models developed was verified at a confidence interval of 95% and 5% significance level with the help of Analysis of Variance (ANOVA). The results of the quadratic order RSM in the form of ANOVA and the corresponding result summary are shown in Tables 6

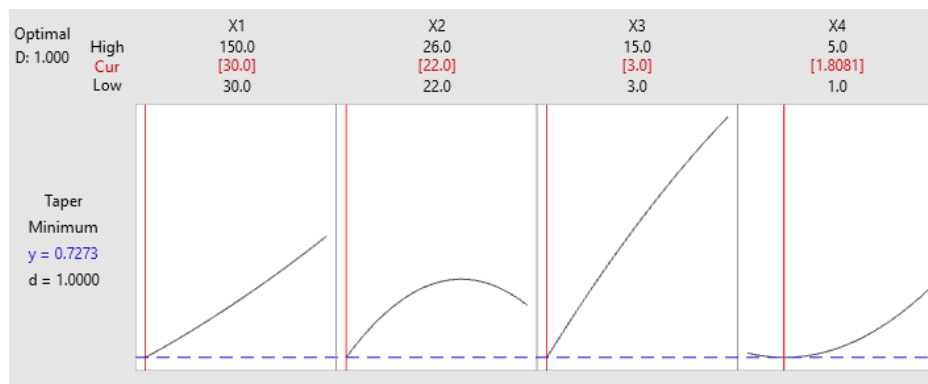


Fig. 5 Optimization plot for taper

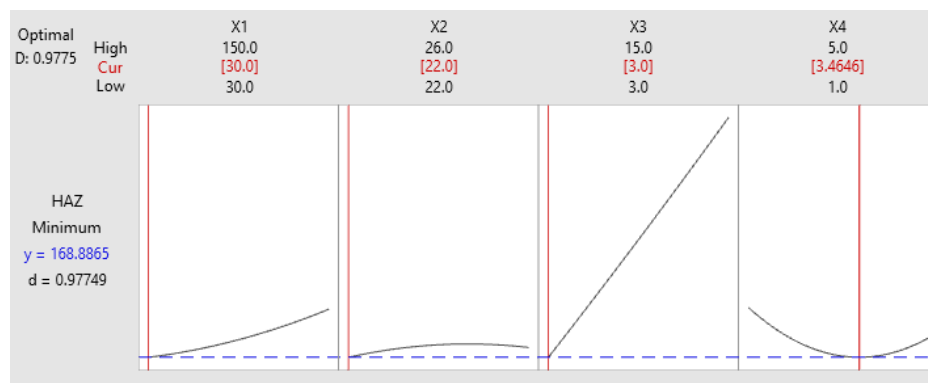


Fig. 6 Optimization plot for HAZ

Table 8 Summary of optimization using RSM methodology

Output parameters	Optimum setting for Control factors				Optimum value
	Cutting Speed (m/s)	Lamp Current (amp)	Pulse frequency (kHz)	Air pressure (kg/cm ²)	
Taper (degree)	30	22	3	1.8081	0.7273
HAZ (μm)	30	22	3	3.4646	168.8865

and 7, respectively. The S value is the error factor and the lesser S value is better. From the above mathematical models, the S values for taper and HAZ were found to be 0.474638 and 58.2713 respectively. The larger the value of R^2 better is the determination of the regression equation coefficient. The imminence of the adjusted R^2 with R^2 decide the fitness of the model.

In addition to the coefficient, a further statistical analysis based on p-value is carried out for their higher-order correlations. It is observed that, most of the parameters (cutting speed, lam current and pulse frequency) have p-values less than 0.05 in case of taper in contrast to the HAZ, which depicts the significance of these parameters on taper. However, the pulse frequency is found to have significant contribution towards HAZ. The same can also be confirmed by the Pareto Chart of the Standardized Effects for taper and HAZ as provided in Fig. 3 and Fig. 4, respectively alongside the respective probability plots. From the probability plots of the output, it is observed that the p-values

are more than 0.2 in both the cases. This indicates that the values obtained from the experiment does not deviate significantly from the mean straight line. Thus, there is no evidence of any non-normality, asymmetry, outliers or unidentified variables existence in this analysis. Also, the data obtained in the regression analysis is following the normal distribution and appears to be a good fit to the currently obtained data.

3.2 Optimization of the responses using desirability approach

The optimization of the desired responses has been carried out using the desirability-based optimization of RSM, which is a unique and powerful optimization technique. At first, individual response optimization for taper and HAZ is performed according to respective objectives (minimization). After that, all the parameters are tuned about their target values to get the parameter settings for the simultaneous optimization of the multiple performances. The measured properties of each expected response are converted into a dimensionless desirability value “ d ” in this desirability function approach. The desirability function has a scale of 0 to 1, with $d=0$ indicating that the response is completely unacceptable and $d=1$ indicating that the response is exactly of the target value (Sahoo and Mishra 2014). The optimization analysis has been carried out using MINITAB statistical software. The optimization plot for the taper shown in Fig. 5, yields the predicted value for minimum taper to be 0.7273 degree for the optimum input parameter setting (cutting speed=30 m/s, lamp current=22amp, frequency=3 kHz and air pressure=1.8081 kg/cm²) with a desirability 1. Similarly, the optimization plot is shown in Fig. 6 with a goal to minimize the HAZ. The predicted value for the minimum HAZ is 168.8865 μm with desirability value 0.97749 and with corresponding optimum input parameter setting (speed=30 m/s, current=22-amp, frequency=3 kHz and air pressure=3.4646 kg/cm²). The optimized value obtained using RSM methodology along with the input parameter setting for individual optimization is also summarized in Table 8 for easy reference.

Moreover, when the optimization for the multiple performances (minimize the taper and HAZ simultaneously) have been performed using the RSM (result shown in Fig. 7), the minimum taper and minimum HAZ values attained are 0.9636 degree and 168.8865 μm , respectively with optimal controllable parameter setting as (speed=30 m/s, current=22-amp, frequency=3 kHz and air pressure=3.4646 kg/cm²) which is analogous to as obtained through individual optimization for the HAZ.

3.3 APSO algorithm

Kennedy and Eberhart developed the basic particle swarm optimization (PSO) in 1995, inspired by swarm behavior in nature such as fish and bird schooling. Extensive studies indicate that PSO is extremely successful for any optimization issues; still, it can often suffer premature convergence for highly multimodal problems. The standard PSO uses the global best g^* as well as the local best x_i^* (Yang et al. 2011) and the search process is based on a deterministic component and a stochastic component. The main objective of using different metaheuristics depends on exploration, exploitation and diversity capability of the algorithm to find out the optimal solution for a single objective and multi-objective optimization problem within the predefined search space. Therefore, various applications of standard PSO and its variants can be found in the literature to estimate exact solutions to tremendously difficult or impossible numeric maximization and minimization problems (Ameur and Assas 2012). However, in standard PSO the local best is used to improve diversity in the solution, but this can be obtained or simulated by using several randomness. There is no justified

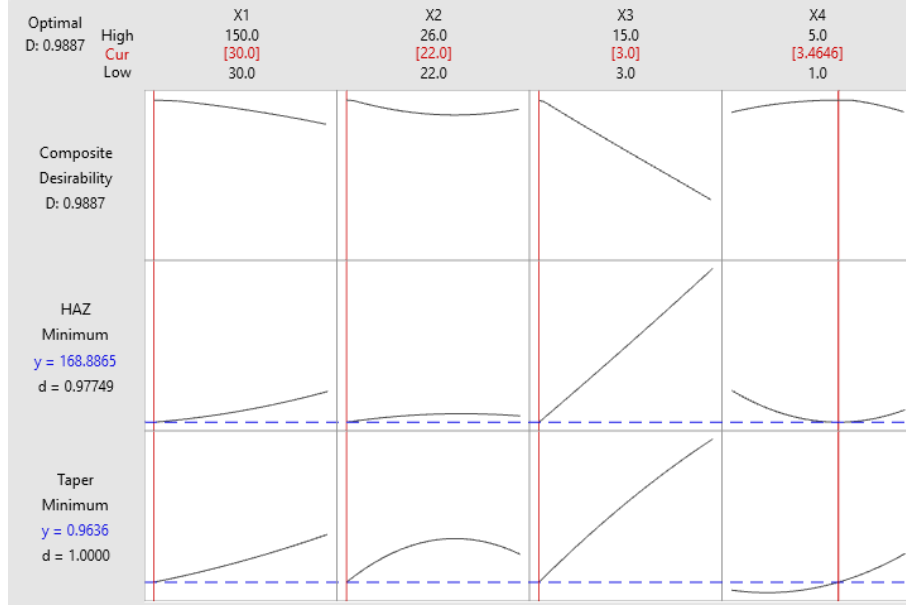


Fig. 7 Optimization plot for all the responses

cause for using the local best instead, if not the optimization issue is strongly nonlinear and multimodal.

Moreover, a simpler version that might speed up the algorithm's convergence is to employ only the global best. In 2008, Yang developed an accelerated particle swarm optimization (APSO), and simpler formula for generating the velocity vector is represented as:

$$v_i^{(t+1)} = v_i^t + \alpha \varepsilon_n + \beta (g^* - x_i^t) \quad (3)$$

To replace the second term in standard PSO, α is drawn from $N(0, 1)$. To improve the convergence characteristics, the update of position in a single step is signified as:

$$x_i^{(t+1)} = (1 - \beta)x_i^t + \beta g^* + \alpha r \quad (4)$$

This simplified version will express the same convergence order. It is worth noting here that in the above equation, the velocity does not appear. So, there is no requirement to initialize the velocity vector. As a result, the APSO is much easier to implement. Here, $(\alpha \times r)$ is the randomization term which gives the process to escape from local minima if α is chosen to be compatible with the scales of the problem of interest, whereas r can be extracted from a probability distribution such as Gaussian. The standard values for this accelerated PSO are $(\alpha=0.1-0.5)$ and $(\beta=0.1-0.7)$ is sufficient for most applications.

As compared to other PSO variants, the APSO algorithm uses only two parameters *i.e.*, α and β . The mechanism is easy to comprehend. Another enhancement to the APSO is to lessen the randomness while the iterations proceed. This means that we can employ a monotonically diminishing function such as $\alpha = \alpha_o e^{(-\gamma t)}$ or $\alpha = \alpha_o \gamma^t$. Where, $\alpha_o=0.5$ to 1, is the initial value of the randomness parameters, t is the number of iterations and γ is the control parameter (value ranges from 0 to 1).

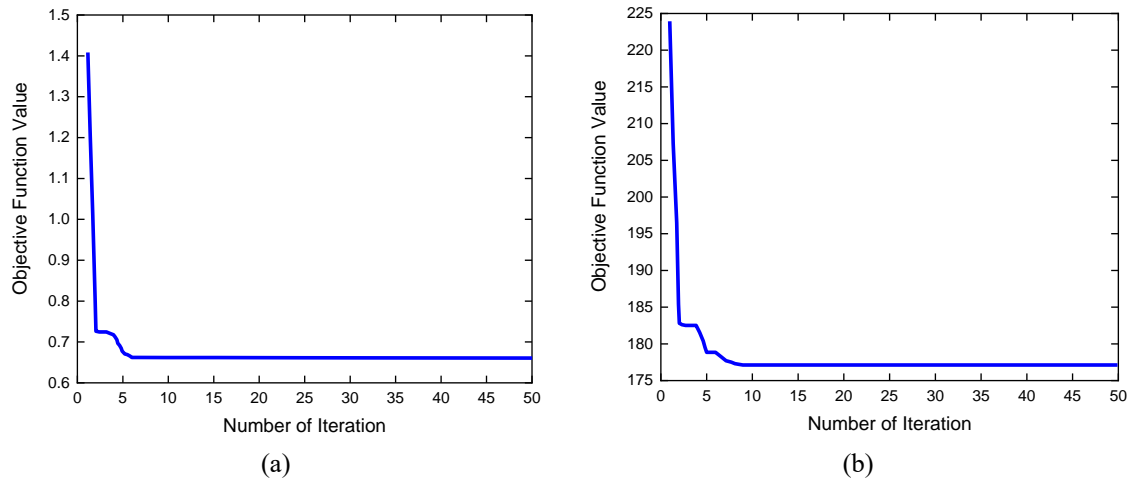


Fig. 8 Convergence of average values of the objective function for (a) Taper, (b) HAZ

Table 9 Optimal solution obtained through APSO for individual responses

Output parameters	Controllable input factors				Optimum value
	Cutting Speed (m/s)	Lamp Current (amp)	Pulse frequency (kHz)	Air pressure (kg/cm ²)	
Taper (degree)	30	22	3	1.8035	0.66096
HAZ (μm)	30	22	3	3.4761	177.18

3.4 Formulation of optimization problem

The goal of the present research work is to identify an optimal setting for process parameters that can minimize both taper and the HAZ of the laser micro-drilling process individually as well as combinedly by implementing the metaheuristic algorithm APSO algorithm.

The single objective function designed for applying the APSO algorithm is represented as,

Minimize (Taper); Minimize (HAZ)

The upper and lower bounds of control parameters are,

$$30 \leq \text{cutting speed} \leq 150, 22 \leq \text{lamp current} \leq 26, 3 \leq \text{pulse frequency} \leq 15, 1 \leq \text{air pressure} \leq 5$$

Such parametric values are indicated as input to the APSO algorithm. The requisite computer code is written in MATLAB environment and used for the computation of the optimum condition of input parameters. In order to determine the efficiency of the APSO algorithm, the convergence behaviour (objective function value versus the number of iterations) of the algorithm is first tested presented in Fig. 8. The corresponding optimal combination of input parameters and the predicted value of minimum taper and minimum HAZ obtained using the APSO algorithm are also shown in Table 9.

3.5 Multi-objective optimization using APSO algorithm

Now, the presently developed APSO algorithm is extended to perform multiple performance characteristic optimization. To do so, the following objective function is built.

Table 10 Results of confirmation experiment

Methodology	Output parameters	Controllable input factors				Optimum value
		Cutting Speed (m/s)	Lamp Current (amp)	Pulse frequency (kHz)	Air pressure (kg/cm ²)	
RSM	Taper (degree)	30	22	3	3.4646	0.9636
	HAZ (μm)					168.8865
APSO	Taper (degree)	30	22	3	2.4045	0.81228
	HAZ (μm)					163.0333
Confirmatory Test	Taper (degree)					0.7942
	HAZ (μm)					162
Improvement w.r.t RSM	Taper (degree)	-	-	-	-	21.33%
	HAZ (μm)					4.25%

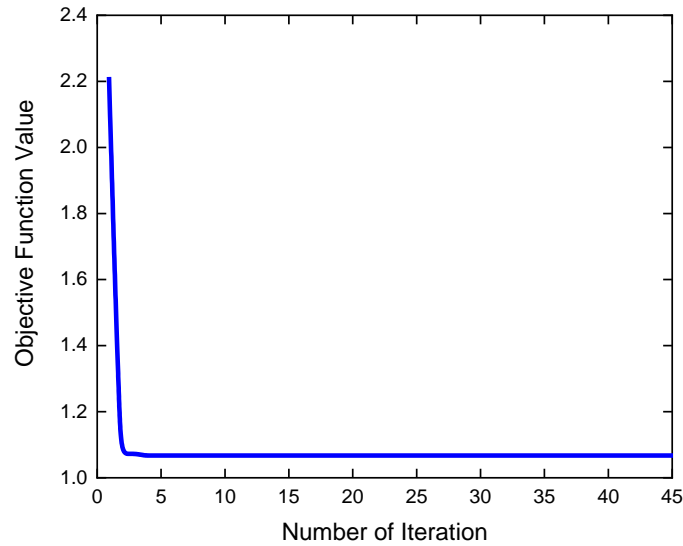


Fig. 9 The objective function in each iteration for multi-objective optimization

$$\text{Min}(Z_1) = \frac{w_1 Y_U(\text{Taper})}{(\text{Taper})_{\min}} + \frac{w_2 Y_U(\text{HAZ})}{(\text{HAZ})_{\min}} \quad (5)$$

Where w_1 and w_2 are the weightage assigned to taper and HAZ, respectively such that $w_1 + w_2 = 1$. Here, equal emphasis (i.e., 50% weightage) is given to each response. The result of the multi-objective optimization of the current laser drilling process is shown in Table 10. The minimum value of the objective function ($Z_1=1.0662$) is obtained from the APSO algorithm for the optimal parameter setting as ($X_1=30$ m/s, $X_2=22$ amp, $X_3=3$ kHz, $X_4=2.4045$ kg/cm²) with the corresponding taper and HAZ values as. The convergence behaviour of the algorithm for the multi-objective optimization has been presented in Fig. 9.

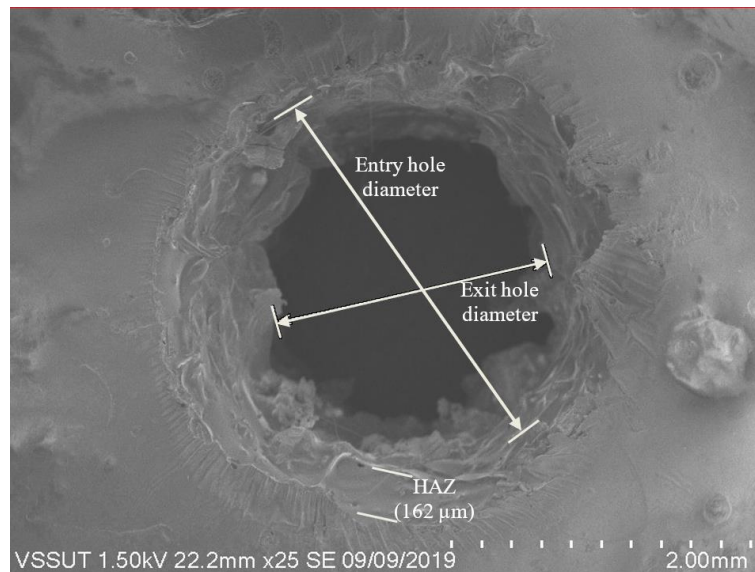


Fig. 10 SEM image of the hole obtained from confirmation test

3.6 Confirmation experiment for multiple performance optimization

The confirmation test is performed with the desired levels of parameters as obtained through APSO and mentioned in Table 10. The confirmation test yields the desired responses as; Taper=0.7942 degree and HAZ=162 μm for which the SEM output is shown in also shown in Fig. 10. From the confirmation results it is observed that the predicted value of Taper and HAZ obtained through RSM methodology have been improved by 21.33% and 4.25% by 25%, respectively by implementing the metaheuristic APSO multi-objective algorithm. Moreover, upon comparing the results provided in Table 10 with those depicted in Table 8 and Table 9, it can be clearly inferred that the currently implemented APSO algorithm has efficiently resulted nondominated solution to the simultaneous optimization problem involving two objective functions (Taper and HAZ) during laser micro-drilling of epoxy based nano composite. The confirmation results demonstrated that the APSO algorithm can be used for optimizing the machining parameters with utmost supremacy.

4. Conclusions

The experimental research work aims to optimize the laser micro drilling parameters of CNT/Epoxy-based polymer matrix nanocomposite by applying Response Surface Methodology and nature-inspired metaheuristics APSO algorithm. The experimental trials are performed as per central composite design and the output responses such as the Taper and HAZ are determined. Nonlinear regression models are used to establish the empirical relationship between control parameters and output responses. Finally, the results of optimized machining parameters are obtained through the RSM as well as the APSO algorithm to minimize both the responses. The findings obtained are then confirmed via the confirmatory test. Based on the experimental result, modeling and optimization of laser drilling parameters the following useful conclusions are drawn:

- The regression models and the Pareto charts depicted that the pulse frequency is found to be the most significant factor for the presently considered output responses.
- The optimal combinations of control factors and the corresponding optimal values for minimum taper and minimum HAZ as obtained through the present APSO agreed well with that attained implementing traditional RSM methodology.
- Although the results obtained via the APSO are very efficient, high-quality solution, and have local exploitation capability, still it is observed that the algorithm suffers from early convergence in the primary stage. So, it is believed that the APSO in combination with newer machine learning algorithms and utilizing other existing versatile optimization techniques can be implemented for comprehensive understanding the selection of appropriate machining conditions and control of various output responses.
- The confirmation result illustrates an improvement of 21.33% and 4.25% in the taper and the HAZ, respectively with respect to the average output values obtained through the traditional RSM methodology.
- Thus, the nature-inspired APSO algorithm is successfully implemented for the optimization of single as well as multi-performance characteristics of laser micro-drilling process for the nanocomposite material. Also, the preservative model based on the RSM methodology is accurate and lead to the improvement in optimal output parameters.
- Although the results obtained from APSO are very efficient, high-quality solution, and have local exploitation capability, still the algorithm suffers from early convergence in the primary stage. So, this study can be extended to further application of APSO in combination with newer machine learning algorithms and utilizing other existing versatile optimization techniques (Teaching learning-based algorithm, water cycle optimization, Firefly algorithm for comprehensive understanding the selection of appropriate machining conditions and control of various output responses. In terms of future work, this study can be extended to analyze the influence of some additional variables, such as study the burr formation, circularity, surface finish of the laser drilled holes.

Acknowledgments

The research described in this paper was financially supported by TEQIP III, VSSUT, Burla (VSSUT/TEQIP/82/2020, dated 20/01/2020 and VSSUT/TEQIP/86/2020, dated 20/01/2020).

References

- Adalarasan, R., Santhanakumar, M. and Thileepan, S. (2017), "Selection of optimal machining parameters in pulsed CO₂ laser cutting of Al₆₀₆₁/Al₂O₃ composite using taguchi-based response surface methodology (T-RSM)", *Int. J. Adv. Manuf. Technol.*, **93**(1-4), 305-317. <https://doi.org/10.1007/s00170-016-8978-5>.
- Ahmed, R.I., Moustafa, M.M., Talaat, A.M. and Ali, W.Y. (2015), "Frictional behaviour of epoxy reinforced copper wires composites", *Adv. Mater. Res.*, **4**(3), 165-178. <https://doi.org/10.12989/amr.2015.4.3.165>.
- Ameur, T. and Assas, M. (2012), "Modified PSO algorithm for multi-objective optimization of the cutting parameters", *Prod. Eng.*, **6**(6), 569-576. <https://doi.org/10.1007/s11740-012-0408-4>.
- Biswas, R., Kuar, A.S., Biswas, S.K. and Mitra, S. (2010), "Artificial neural network modelling of Nd:YAG laser microdrilling on titanium nitride-alumina composite", *Int. J. Adv. Manuf. Technol.*, **224**(3), 473-482. <https://doi.org/10.1243/09544054JEM1576>.

- Chatterjee, S., Mahapatra, S.S., Bharadwaj, V., Choubey, A., Upadhyay, B.N. and Bindra, K.S. (2018), "Quality evaluation of micro drilled hole using pulsed Nd:YAG Laser: A case study on AISI 316", *Lasers Manuf. Mater.*, **5**(3), 248-269. <https://doi.org/10.1007/s40516-018-0067-1>.
- Chien, W.T. and Hou, S.C. (2007), "Investigating the recast layer formed during the laser trepan drilling of inconel 718 using the Taguchi method", *Int. J. Adv. Manuf. Technol.*, **33**(3-4), 308-316. <https://doi.org/10.1007/s00170-006-0454-1>.
- Ciurana, J., Arias, G. and Ozel, T. (2009), "Neural network modeling and particle swarm optimization (PSO) of process parameters in pulsed laser micromachining of hardened AISI H13 steel", *Mater. Manuf. Pr.*, **24**(3), 358-368. <https://doi.org/10.1080/10426910802679568>.
- Galińska, A. (2020), "Mechanical joining of fibre reinforced polymer composites to metals - A review Part i: Bolted joining", *Polym.*, **12**(10), 1-48. <https://doi.org/10.3390/polym12102252>.
- Gao, J.G., Zhai, D. and Wu, W.H. (2014), "Preparation and characterization of boron-nitrogen coordination phenol resin/SiO₂ nanocomposites", *Adv. Mater. Res.*, **3**(1), 259-269. <https://doi.org/10.12989/amr.2014.3.1.259>.
- Gauri, S.K. and Pal, S. (2010), "Comparison of performances of five prospective approaches for the multi-response optimization", *Int. J. Adv. Manuf. Technol.*, **48**(9-12), 1205-1220. <https://doi.org/10.1007/s00170-009-2352-9>.
- Gautam, G.D. and Mishra, D.R. (2019), "Firefly algorithm based optimization of kerf quality characteristics in pulsed Nd : YAG laser cutting of basalt fiber reinforced composite", *Compos. Part B: Eng.*, **176**, 107340. <https://doi.org/10.1016/j.compositesb.2019.107340>.
- George, S.M., Puglia, D., Kenny, J.M., Causin, V., Parameswaranpillai, J. and Thomas, S. (2013), "Morphological and mechanical characterization of nanostructured thermosets from epoxy and styrene-block-butadiene-block-styrene triblock copolymer", *Indust. Eng. Chem. Res.*, **52**(26), 9121-9129. <https://doi.org/10.1021/ie400813v>.
- Goswami, D. and Chakraborty, S. (2015), "A Study on the optimization performance of fireworks and cuckoo search algorithms in laser machining processes", *J. Inst. Eng. Ser. C*, **96**(3), 215-229. <https://doi.org/10.1007/s40032-014-0160-y>.
- Jain, A., Singh, B. and Shrivastava, Y. (2019), "Reducing the heat-affected zone during the laser beam drilling of basalt-glass hybrid composite", *Compos. Part B: Eng.*, **176**, 107294. <https://doi.org/10.1016/j.compositesb.2019.107294>.
- Kipfer, B.A. (2021), "Mont", *Encyclopedic Dictionary of Archaeology*, Springer International Publishing, Cham, Switzerland.
- Kuar, A.S., Dhara, S.K. and Mitra, S. (2010), "Multi-response optimisation of Nd:YAG laser micro-machining of die steel using response surface methodology", *Int. J. Manuf. Technol. Manag.*, **21**(1-2), 17-29. <https://doi.org/10.1504/IJMTM.2010.034283>.
- Kuar, A.S., Biswas, P., Mitra, S. and Biswas, R. (2008), "Experimental investigation of Nd: YAG laser micro-grooving operation of alumina workpiece using RSM", *Int. J. Mater. Struct. Integr.*, **1**(4), 355-370. <https://doi.org/10.1504/IJMSI.2008.019618>.
- Kumar, D. and Gururaja, S. (2020), "Investigation of hole quality in drilled Ti/CFRP/Ti laminates using CO₂ laser", *Opt. Laser Technol.*, **126**, 106130. <https://doi.org/10.1016/j.optlastec.2020.106130>.
- Liu, C., Zhang, X., Gao, L., Jiang, X., Li, C. and Yang, T. (2021), "Feasibility of micro-hole machining in fiber laser trepan drilling of 2.5D Cf/SiC composite: experimental investigation and optimization", *Opt.*, **242**, 167186. <https://doi.org/10.1016/j.ijleo.2021.167186>.
- Masir, A.N., Darvizeh, A. and Zajkani, A. (2018), "Mechanical properties of top neck mollusks shell nano composite in different environmental conditions", *Adv. Mater. Res.*, **7**(3), 185-194. <https://doi.org/10.12989/amr.2018.7.3.185>.
- Meijer, J. (2004), "Laser beam machining (LBM), state of the art and new opportunities", *J. Mater. Pr. Technol.*, **149**(1-3), 2-17. <https://doi.org/10.1016/j.jmatprotec.2004.02.003>.
- Mishra, D.R., Bajaj, A. and Bisht, R. (2020), "Optimization of multiple kerf quality characteristics for cutting operation on carbon-basalt-kevlar29 hybrid composite material using pulsed Nd:YAG laser using GRA", *CIRP J. Manuf. Sci. Technol.*, **30**, 174-183. <https://doi.org/10.1016/j.cirpj.2020.05.005>.

- Mukherjee, R., Goswami, D. and Chakraborty, S. (2013), "Parametric optimization of Nd : YAG laser beam machining process using artificial bee colony algorithm", *J. Indust. Eng.*, **2013**, 570250. <https://doi.org/10.1155/2013/570250>.
- Muthukumar, V., Suresh Babu, A., Venkatasamy, R. and Senthil Kumar, N. (2015), "An accelerated particle swarm optimization algorithm on parametric optimization of WEDM of die-steel", *J. Inst. Eng. Ser. C*, **96**(1), 49-56. <https://doi.org/10.1007/s40032-014-0143-z>.
- Nagesh, S., Narasimha Murthy, H.N., Krishna, M. and Basavaraj, H. (2013), "Parametric study of CO2 laser drilling of carbon nanopowder/vinylester/glass nanocomposites using design of experiments and grey relational analysis", *Opt. Laser Technol.*, **48**, 480-488. <https://doi.org/10.1016/j.optlastec.2012.11.013>.
- Patel, P., Gohil, P. and Rajpurohit, S. (2013), "Laser machining of polymer matrix composites: Scope, limitation and application", *Int. J. Eng. Trends Technol.*, **4**(6), 2391-2399.
- Rajesh, P., Nagaraju, U., Harinath Gowd, G. and Vishnu Vardhan, T. (2017), "Experimental and parametric studies of Nd:YAG laser drilling on austenitic stainless steel", *Int. J. Adv. Manuf. Technol.*, **93**(1-4), 65-71. <https://doi.org/10.1007/s00170-015-7639-4>.
- Rao, R. and Yadava, V. (2009), "Multi-objective optimization of Nd:YAG laser cutting of thin superalloy sheet using grey relational analysis with entropy measurement", *Opt. Laser Technol.*, **41**(8), 922-930. <https://doi.org/10.1016/j.optlastec.2009.03.008>.
- Sahoo, A. and Mishra, P. (2014), "A response surface methodology and desirability approach for predictive modeling and optimization of cutting temperature in machining hardened steel", *Int. J. Indust. Eng. Comput.*, **5**(3), 407-416. <https://doi.org/10.5267/j.ijiec.2014.4.002>.
- Saini, S.K. and Dubey, A.K. (2019), "Study of material characteristics in laser trepan drilling of ZTA", *J. Manuf. Pr.*, **44**, 349-358. <https://doi.org/10.1016/j.jmapro.2019.06.017>.
- Sharon, M., Nandgavkar, I. and Sharon, M. (2017), "Platinum nanocomposites and its applications: A review", *Adv. Mater. Res.*, **6**(2), 129-153. <https://doi.org/10.12989/amr.2017.6.2.129>.
- Sibaliija, T.V., Petronic, S.Z., Majstorovic, V.D., Prokic-Cvetkovic, R. and Milosavljevic, A. (2011), "Multi-response design of Nd:YAG laser drilling of ni-based superalloy sheets using taguchi's quality loss function, multivariate statistical methods and artificial intelligence", *Int. J. Adv. Manuf. Technol.*, **54**(5-8), 537-552. <https://doi.org/10.1007/s00170-010-2945-3>.
- Singh, N. and Aul, G.D. (2021), "Development of cobalt coated mwcnts/polyurethane composite for microwave absorption", *Adv. Mater. Res.*, **10**(3), 195-209. <https://doi.org/10.12989/amr.2021.10.3.195>.
- Suhaimi, S.N., Shamsuddin, S.M., Ahmad, W.A., Hasan, S. and Venil, C.K. (2019), "Comparison of particle swarm optimization and response surface methodology in fermentation media optimization of flexirubin production", *J. Teknol.*, **81**(2), 53-60. <https://doi.org/10.11113/jt.v81.10766>.
- Wang, Q. and G. Chen. (2014), "Effect of pre-treatment of nanofillers on the dielectric properties of epoxy nanocomposites", *Adv. Mater. Res.*, **21**(4), 1809-1816. <https://doi.org/10.1109/TDEL.2014.004278>.
- Yan, Y., Ji, L., Bao, Y. and Jiang, Y. (2012), "An experimental and numerical study on laser percussion drilling of thick-section alumina", *J. Mater. Pr. Technol.*, **212**(6), 1257-1270. <https://doi.org/10.1016/j.jmatprotec.2012.01.010>.
- Yang, X.S., Deb, S. and Fong, S. (2011), "Accelerated particle swarm optimization and support vector machine for business optimization and applications", *Networked Digital Technologies: Third International Conference, NDT 2011*, Macau, China, July.